Bioelectrochemistry 147 (2022) 108176

Contents lists available at ScienceDirect

Bioelectrochemistry

journal homepage: www.journals.elsevier.com/bioelectrochemistry

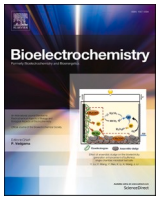

Electrochemical DNA biosensor for chronic myelocytic leukemia based on hybrid nanostructure

Karen Y.P.S. Avelino [a,b], Léony S. Oliveira [a,b], Maryana R. Santos [b], Norma Lucena-Silva [c,d], César A.S. Andrade [a,b], Maria D.L. Oliveira [a,b,*]

[a] Programa de Pós-Graduação em Inovação Terapêutica, Universidade Federal de Pernambuco, 50670-901 Recife, PE, Brazil
[b] Laboratório de Biodispositivos Nanoestruturados, Departamento de Bioquímica, Universidade Federal de Pernambuco, 50670-901 Recife, PE, Brazil
[c] Instituto Aggeu Magalhães, Fundação Oswaldo Cruz (Fiocruz), 50670-420 Recife, PE, Brazil
[d] Laboratório de Biologia Molecular, Departamento de Oncologia Pediátrica, Instituto de Medicina Integral Professor Fernando Figueira (IMIP), 50070-550 Recife, PE, Brazil

ARTICLE INFO

Keywords:
Biosensor
Hybrid nanocomposite
BCR/ABL fusion gene
Polypyrrole
Zinc oxide
Electrochemistry

ABSTRACT

The present research refers to elaborating a new label-free electrochemical biosensor used to detect the BCR/ABL fusion gene. We used a hybrid nanocomposite composed of chitosan and zinc oxide nanoparticles (Chit-ZnONP) immobilized on a polypyrrole (PPy) film. DNA segments were covalently immobilized, allowing biomolecular recognition. Atomic force microscopy (AFM), cyclic voltammetry (CV), and electrochemical impedance spectroscopy (EIS) were used to evaluate the assembly stages of the biosensor. The biosensor's analytical performance was investigated using recombinant plasmids containing the target oncogene and clinical samples from patients with chronic myeloid leukemia (CML). A limit of detection (LOD) of 1.34 fM, limit of quantification (LOQ) of 4.08 fM, and sensitivity of 34.03 μA fM^{-1} cm^2 were calculated for the BCR/ABL fusion oncogene. The sensing system exhibited high specificity, selectivity, and reproducibility with a standard deviation (SD) of 4.21%. Additionally, a linear response range was observed between 138.80 aM to 13.88 pM with a regression coefficient of 0.96. Also, the biosensor shows easy operationalization and fast analytical response, contributing to the early cancer diagnosis. The proposed nanostructured device is an alternative for the genetic identification BCR/ABL fusion gene.

1. Introduction

Genetic disorders cause Leukemias in hematopoietic precursor cells. Leukemic diseases form a heterogeneous group of neoplasms that constitute one of the most prevalent types of hematologic cancer worldwide. The BCR/ABL fusion gene, which characterizes the Philadelphia chromosome, is predominant in CML patients, constituting an essential genetic biomarker for oncogenesis. The formation of this hybrid oncogene results from the rearrangement between the ABL sequence of chromosome 9 and the breakpoint cluster region (BCR) of chromosome 22 [1,2]. In this perspective, efficient molecular diagnosis with rapid identification of the BCR/ABL fusion gene is essential for patients with suspected leukemia, allowing an early diagnosis, better stratification of the disease according to risk, and prescription of specific therapies [3].

The presumptive methods for identifying CML-related genetic abnormalities are based on cytogenetic studies, fluorescent in situ hybridization (FISH), and quantitative reverse transcription-polymerase chain reaction (qRT-PCR). Although these techniques are effective for the diagnosis, there are still limiting factors, protocols lasting 24 to 48 h for metaphase analysis in cytogenetic assessments, overlapping of chromosome bands in FISH and variable selectivity in RTq-PCR assays. Moreover, there is a need for qualified professionals, robust equipment, and, frequently, simultaneous use of different techniques for the accurate confirmation of the Philadelphia chromosome, generating counterpoints that increase the cost and diagnostic response time [4].

The bioanalysis procedure is based on molecular hybridization between complementary oligonucleotide fragments anchored on transducer surfaces [5]. Thus, DNA biosensors provide selective and specific detection of target genes quickly and inexpensively. Electrochemical biosensors become even more advantageous due to enhanced output performance, high sensitivity, and the possibility of label-free response

* Corresponding author at: Departamento de Bioquímica, UFPE, 50670-901 Recife, PE, Brazil.
E-mail address: maria.dloliveira@ufpe.br (M.D.L. Oliveira).

https://doi.org/10.1016/j.bioelechem.2022.108176
Received 21 February 2022; Received in revised form 3 June 2022; Accepted 4 June 2022
Available online 8 June 2022

analysis. However, the influence of experimental factors needs to be investigated for bioanalytical success, such as biomolecules concentration, hybridization time, temperature, pH, and presence of salts. Some of these factors, such as pH and temperature, can directly affect the stability and conformation of DNA probes. Specifically, sugar residues and phosphate groups of nucleic acids can be altered by ionic strength, causing loss of oligonucleotide integrity [6].

Nanostructures and functional materials have been associated with the development of electrochemical interfacing platforms [7]. PPy is a organic polymer with highlighted conductivity. The molecular structure of PPy enables an easy doping process, substantially increasing the material's conductivity through the formation and movement of polarons and bipolaron. Another advantage of applying PPy in electrochemical biosensors is its direct synthesis by electropolymerization on the electrode surface, allowing an experimental control of the polymeric film thickness. The association of conductive polymer and nanostructure metal oxides has received significant attention [8].

Zinc oxide nanoparticles (ZnONPs) are semiconductor material that exhibits outstanding properties such as physical and chemical stabilities, high electron mobility, and high surface area for molecules immobilization [9,10]. ZnONPs associated with Pd and Pt [11], gold [12], chitosan (Chit) [13], polyaniline, and carbon nanotubes have been used to manufacture diagnostic devices [14]. Chit is a high molecular weight polysaccharide obtained from chitin that has been used to synthesize multilayer structures and hybrid nanocomposites [15]. Chit provides a highly favorable microenvironment for immobilizing biomolecules without loss of biological activity [16].

The development of new sensors utilizing nanomaterials for real-time bioanalysis is essential for the molecular detection of genetic biomarkers. In this perspective, Shamsipur et al. [17] created a DNA biosensor based on graphene nanosheets stabilized by hemoglobin@gold nanoclusters for the electrochemical detection of short DNA species. The BCR/ABL fusion gene was identified in a concentration range of 0.1 fM to 10 pM with a LOD of 0.037 fM, using methylene blue as a signaling probe. 3D corals based on polyaniline nanostructures were developed to capture the BCR/ABL fusion gene, through the use of DNA probes. The gene was quantified with high sensitivity (LOD of 7aM) in clinical samples [18]. Electrostatically immobilized oligonucleotides on zinc oxide nanorods were obtained for impedimetric determination of BCR/ABL fusion gene [19]. The sensing tool displayed a dynamic range from 1.0 pM to 1.0 nM with a LOD of 0.275 pM. Due to the high prevalence of CML among hematologic malignancies, alternative methods for molecular screening of the BCR/ABL chimeric oncogene should be considered.

The present study reports an electrochemical DNA biosensor as an innovative tool for analyzing and detecting the CML genetic biomarker. The sensing system based on Chit-ZnONP hybrid nanostructures and PPy polymer enabled the BCR/ABL fusion gene identification with high analytical quality, sensitivity, selectivity, and reproducibility. The recognition of the molecular hybridization in clinical samples configured the biosensor as an alternative for medical diagnosis for patients with malignant hematologic disorders. In addition to the early diagnosis of leukemia, the electrochemical test can contribute in an innovative way to the screening of minimal residual disease and evaluation of the therapeutic effectiveness.

2. Materials and methods

2.1. Reagents

Pyrrole (98%), ZnONps (<50 nm) (97%), Chit (75–85%), hydrochloric acid (HCl) (37%), glacial acetic acid ($C_2H_4O_2$) (≥99.7%), glutaraldehyde (25%), bovine serum albumin (BSA) (≥98%), potassium ferricyanide ($K_3[Fe(CN)_6]$) (≥99.0%), potassium ferrocyanide ($K_4[Fe(CN)_6]$) (98.5–102.0%), sodium phosphate monobasic and dibasic (≥99.0%), 0.05 μm alumina paste (α-Al_2O_3) were obtained from Sigma Aldrich Co. (St Louis, USA). Trizol was acquired from Invitrogen Co. Ltd. (Carlsbad, CA, USA). The ultrapure water resulting from a Milli-Q Plus purification system (Billerica, USA) was used to prepare analytical grade solutions.

2.2. Oligonucleotide probes and real samples

Conventional PCR and agarose gel electrophoresis in the presence ethidium bromide evaluated the clinical and plasmid samples. The recombinant plasmid containing the BCR/ABL fusion gene was amplified using the ALL and CML primers: ALL (9;22) 5′-AGATACTCAGCGGCATTG-3′ and CML (9;22) 5′-AGCTTCTCCCTGACATCCGTG-3′ primers [20]. Subsequently, chimeric DNA sequences were cloned into the pTA vector. Thus, the analytical results of the biosensor were validated against a standard diagnostic method.

Patients with a leukemia diagnosis were submitted to iliac bone aspiration. The clinical samples were collected with patients' informed consent from the Pediatric Oncology Service biorepository at the Integral Medicine Institute Prof. Fernando Figueira. Bone marrow samples from unselected patients were subjected to genetic analysis after total RNA extraction in 5×10^6 cells using Trizol reagent. Reverse transcription to obtain cDNA specimens was processed using an oligonucleotide primer. This study was approved by the Research Ethics Committee of the Aggeu Magalhães Institute (FIOCRUZ Pernambuco) with the Certificate of Presentation for Ethical Appreciation (CAAE) no. 13296913.3.0000.5190.

2.3. Synthesis of the Chit-ZnONP nanocomposite and construction of the nanostructured biosensor

The methodology adapted for the synthesis of the Chit-ZnONP nanocomposite was based on Xin et al, 2010 [21] and Rovina and Siddiquee, 2016 [22]. Chit and ZnONPs solutions were prepared at a 1 mg/mL concentration in a 1% acetic acid. Subsequently, the final mixture (volumetric ratio of 1:1) was stirred by magnetic conduction for 30 min at room temperature, then ultrasonication for approximately 1 h.

Preliminarily, the bare gold electrode was moderately polished with an alumina suspension (Al_2O_3) with a particle size of 0.05 μm. Afterward, it was rinsed with ultrapure water, submitted to an ultrasound bath for 10 min to remove residual particles, and dried in air. The first stage of the sensing platform corresponds to the electrochemical polymerization of PPy using 20 mL of 0.5 M HCl solution containing 30 mM pyrrole monomer. Six voltammetric cycles were performed in a potential range of −0.4 at + 1.0 V at a scan rate of 100 mV s^{-1}. The second stage refers to the adsorption of the Chit-ZnONP hybrid nanocomposite on the polymeric film. In this second stage, 2 μL of the colloidal solution was added for 30 min to obtain a self-assembled nanostructured layer. The third stage consists of the biofunctionalization of the PPy/Chit-ZnONP interface platform with DNA probes to identify the BCR/ABL fusion oncogene. The immobilization of oligonucleotide sequences was performed by dropping 0.5% glutaraldehyde (v = 2 μL) with an incubation time of 15 min. Subsequently, 2 μL of a 25 pmol/μL DNA solution were added for biomolecular conjugation. Glutaraldehyde is a functional crosslinking agent to bind amino groups of the Chit and functionalized DNA. Finally, the fourth stage comprises blocking the sensor layer's nonspecific sites with BSA protein. In this step, 2 μL of 1% BSA solution (pH 7.4) were incorporated over the electrode surface to obtain the PPy/Chit-ZnONP/Probe/BSA system (Scheme 1).

2.4. Studies of genetic detection

The sensitivity and specificity of the electrochemical biosensor were assessed through hybridization studies with recombinant plasmids containing the BCR/ABL chimeric oncogene in variable concentrations (13.88 pM to 138.80 aM). In addition, clinical specimens (cDNA samples) from patients with Philadelphia chromosome (Ph)-positive chronic

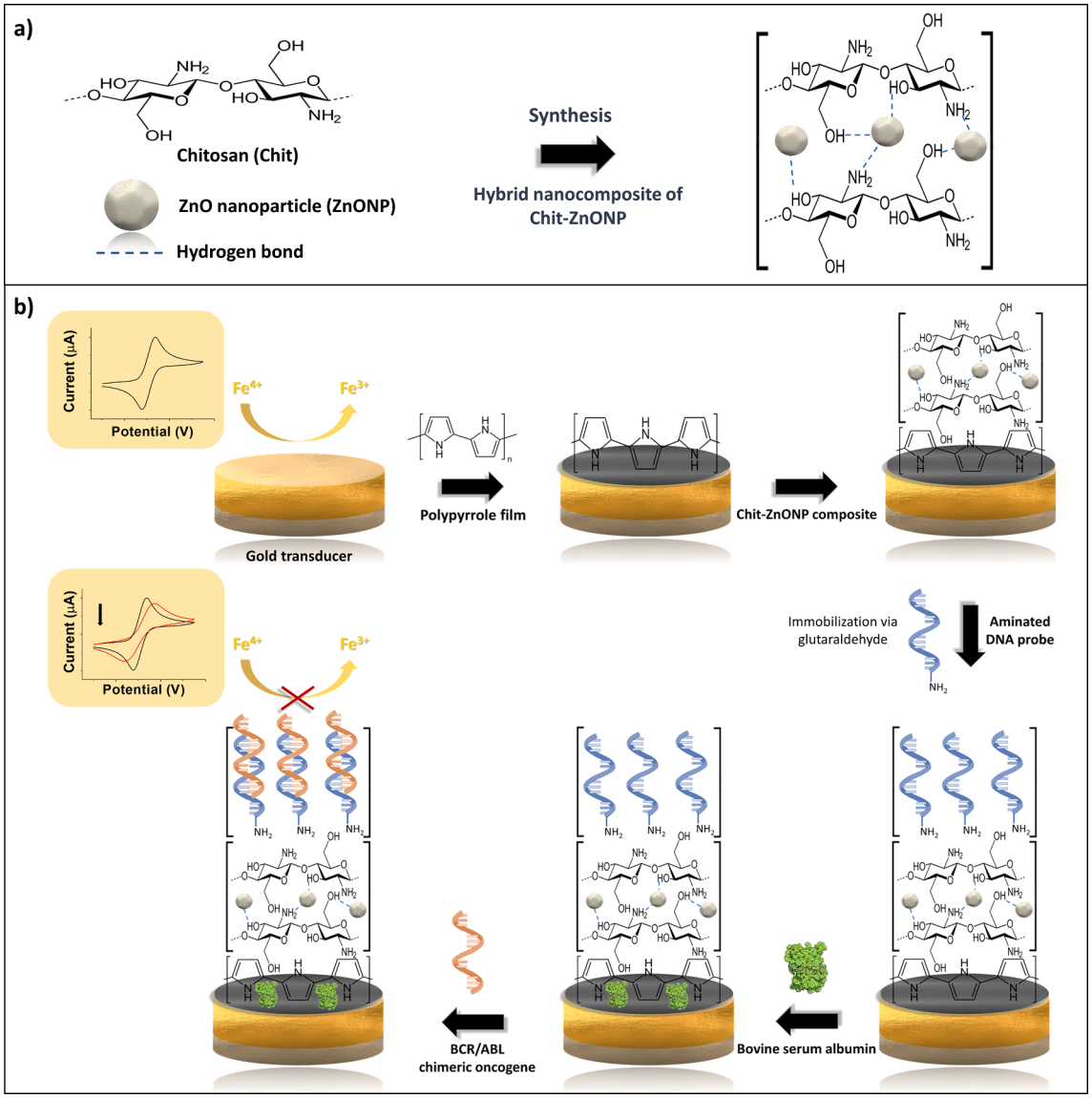

Scheme 1. Representation of the Chit-ZnONP hybrid nanocomposite (a) and its use in a nanostructured biosensor based on polypyrrole (PPy), Chit-ZnONP, DNA probe, and bovine serum albumin (BSA) for the detection of the BCR/ABL chimeric oncogene.

myelogenous leukemia were also used for the genetic screening. The biosensor was exposed to 2 μL of the sample for 15 min to the biorecognition process. The temperature of 94 °C was used to cause the denaturation of the genetic material before the biorecognition assay. Dilutions of all biological samples were prepared with phosphate buffer saline solution (PBS, 10 mM, pH 7.4) and kept frozen.

2.5. Electrochemical measurements

An Autolab PGSTAT 128 N in potentiostatic mode (MetrohmAutolab Inc., Netherlands) controlled by NOVA 1.11 software was employed in the electroanalytical measurements. An electrochemical cell was used in conventional configuration with three electrodes immersed in support electrolyte of PBS (10 Mm, pH 7.4) containing 10 mM $K_4[Fe(CN)_6]$/$K_3[Fe(CN)_6]$ (1:1, v/v). A modified gold electrode ($\phi = 2$ mm) was used as a working electrode. Ag/AgCl saturated with 3 M KCl and platinum wire were used as reference and counter electrodes. Cyclic voltammograms for interfacial characterization were obtained from the application of potentials between −0.2 and +0.7 V with a sweep rate of 50 mV s^{-1}. Cole-Cole diagrams were recorded in a frequency range of 100 mHz to 100 kHz using a potential of 10 mV and integration time of 0.125 s. The electrochemical analysis was obtained at least three independent repetitions of the experiment at room temperature and inside a Faraday cage.

2.6. Microscopy measurements

The morphological characterization of the biosensor construction and its interactions with the BCR/ABL oncogene was performed using an atomic force microscope (SPM-9500; Shimadzu Corporation, Tokyo, Japan). AFM cantilevers with aluminum-coated silicon probe (Nanoworld, Japan; resonant frequency = 300 kHz; force constant = 42 N. m^{-1}) were used noncontact mode at room temperature. The topographic micrographs (512 points per line) were collected in a scan area of 5 × 5 μm. Finally, the 3D images were processed and analyzed using the Gwyddion software.

3. Results and discussion

3.1. Microscopic characterization

AFM was employed to monitor biosensor surface morphologies and

investigate biomolecular activities against clinical samples with a positive diagnosis for the BCR/ABL chimeric oncogene. The PPy electrochemical synthesis resulted in a nodular polymeric matrix with an average thickness of 125 nm (Fig. 1a). PPy globular nodules are expected in electropolymerized thin films, contributing to electrolyte permeation and higher electric conductivity [23]. These structures are dependent on the oxidation–reduction states of the polymer, pyrrole concentration, properties of the doping ions, polymer film thickness, and experimental conditions of electrochemical polymerization [24]. Metal oxide nanoparticles were homogeneously deposited on the PPy polymer, where the PPy/ZnONP film has a maximum height of 201 nm (Fig. 1b). For comparison of the topographic profile, when ZnONPs are in the form of a hybrid nanocomposite with the Chit biopolymer, an increase in surface heterogeneity can be verified (Fig. 1c). Topographic peaks of up to 218 nm were evidenced after the self-assembly of the Chit-ZnONP nanocomposite on the polymeric substrate. The height difference of the PPy and PPy/Chit-ZnONP films suggests that the hybrid nanomaterial has an approximate diameter of 93 nm.

The chemical anchorage of the DNA probe on the PPy/Chit-ZnONP nanoplatform was mediated through glutaraldehyde. Sequentially, incorporating BSA globular proteins enabled the blocking of non-functional sites on the transducer. The AFM 3D image (Fig. 1d) showed that the PPy/Chit-ZnONP/Probe/BSA biosensing system is characterized by well-defined peaks and valleys with a maximum height of 0.24 μm. The flattening structural feature in Fig. 1e indicates the biomolecular hybridization process after exposure of the biosensor to positive CML sample. When the biosensor was exposed to the BCR/ABL oncogene during the biorecognition assay, there was an increase of 0.11 μm in the surface roughness measurements with a maximum height of 0.35 μm. Distinctively, Fig. 1f shows a granular topology with a maximum peak of 0.21 μm for the sensor platform during selectivity tests with a negative sample of CML.

3.2. Electrochemical characterization of the genetic sensing platform

3.2.1. Impedimetric characterization

The physical–chemical analysis of the DNA biosensor preparation stages is shown in Fig. 2. Nyquist plots were adopted to display the EIS data. The Randles circuit model was employed to fit and interpret the experimental spectra accurately (inset of Fig. 2a). This equivalent circuit is composed of a constant phase element (CPE) related to the charge concentration on the electric double layer; resistance to charge transfer (R_{CT}) associated with electron flow between the electrode and electrolytes in solution; the resistance of the electrolyte solution (R_S); and Warburg impedance (Z_W). The impedimetric parameters were summarized in the supplementary material (Table S1).

The impedimetric investigation for bare gold electrode (Fig. 2a and Fig. S1) showed an almost linear response characterized by a low R_{CT} value ($R_{CT} = 0.15 \pm 0.001$ kΩ). The decrease of electrochemical resistance from 0.15 ± 0.001 kΩ (for gold electrode) to 0.01 ± 0.0001 (for PPY-modified gold electrode) confirmed the presence of the polymeric film on the metallic surface. These results suggest that the PPy polymer can improve the charge-transfer efficiency of bioanalytical devices, thus favoring the chemical stability, sensitivity, and selectivity of sensing tools [25].

Reduced charge transfer in the electric double layer was observed ($R_{CT} = 2.02 \pm 0.07$ kΩ) after electrodic modification with the Chit-ZnONP nanocomposite. The conjugation of the Chit-ZnONP hybrid material on the PPy polymer favors the increase in the surface area, provides chemical groups (–NH_2 and –OH) for the covalent immobilization of oligonucleotides, and offers a hydrophilic and biocompatible microenvironment, necessary for the maintenance of the molecular conformation of immobilized biomolecules.

The biofunctionalization of the PPy/Chit-ZnONP nanostructured platform with oligonucleotide probes caused a reduction in the impedimetric signal ($R_{CT} = 10.86 \pm 0.15$ kΩ). This phenomenon is related to the reduced accessibility of redox probe in the sensor system due to the electrostatic repulsion between the phosphate groups of the DNA probes and the negative charges of the $[Fe(CN)_6]_{3-}/[Fe(CN)_6]_{4-}$ ions. Consequently, the partial impediment of the oxidation–reduction reactions in the regions adjacent to the electrode surface is favored [41]. Additionally, BSA caused an increase in resistance ($R_{CT} = 12.56 \pm 0.45$ kΩ).

3.2.2. Voltammetric characterization

Cyclic voltammograms are graphical representations of a current (I) measured as a function of a linearly swept potential (E) in the form of a triangular wave. Valuable parameters can be obtained from electroanalytical analysis, such as anodic peak current (Ipa), cathodic peak current (Ipc), anodic peak potential (Epa), and cathodic peak potential (Epc). These variables provide information about charge transfer kinetics, reversibility of electrochemical reactions, redox potentials of

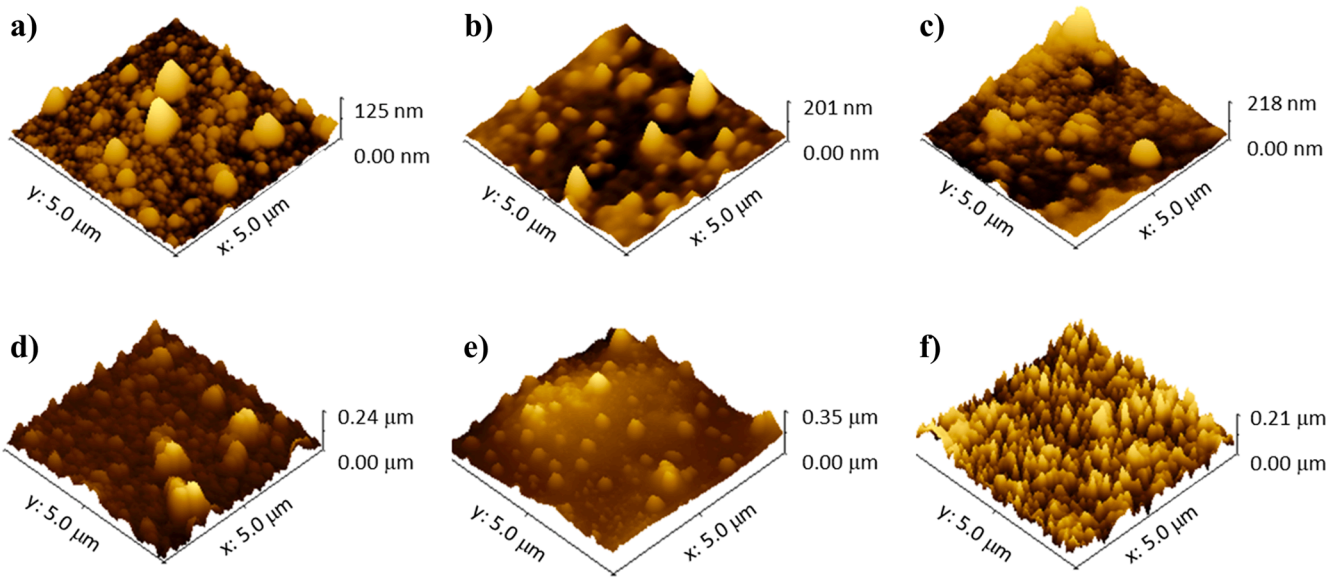

Fig. 1. Atomic force microscopy (AFM) images for PPy (a); PPy/ZnONP (b); PPy/Chit-ZnONP (c); PPy/Chit-ZnONP/Probe/BSA (d); Biosensor/CML positive sample (e); and Biosensor/CML negative sample (f).

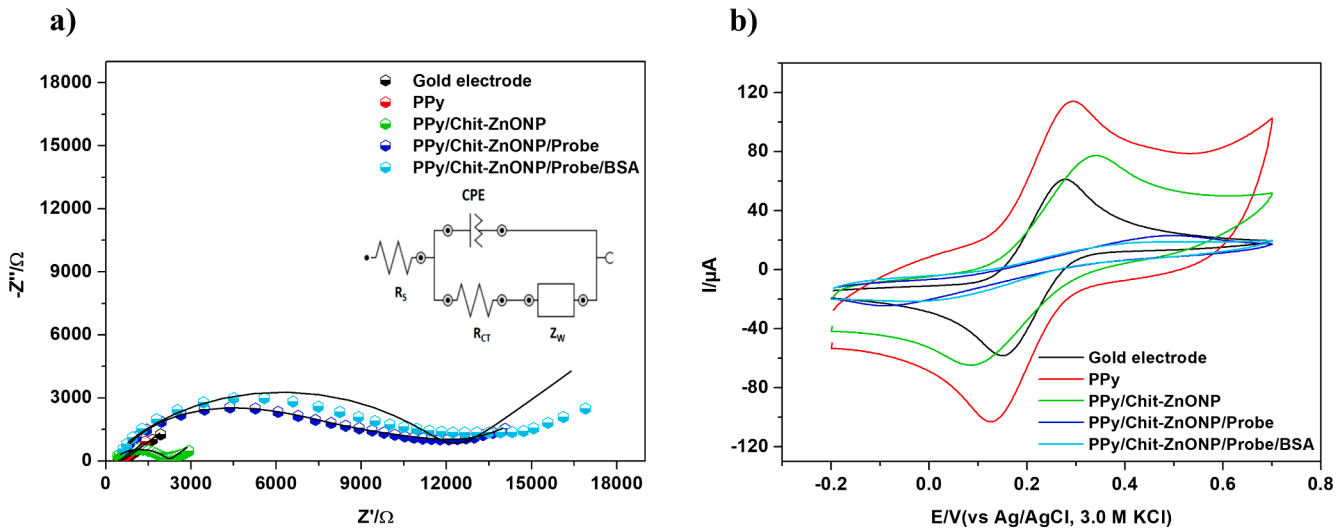

Fig. 2. Impedance spectra (a) and cyclic voltammograms (b) for each assembly step of the nanostructured biosensor based on PPy/Chit-ZnONP/Probe/BSA. Inset: Equivalent circuit used to adjust impedance measurements (a). Three consecutive analyzes were conducted in each methodological procedure, where the experimental values are displayed as the mean values ± standard deviation.

electroactive substances, biomolecular interactions, and surface modification processes [26].

Voltammetric measurements were recorded in 10 mM $[Fe(CN)_6]^{3-/4-}$ solution (Fig. 2b). As expected, the voltammetric responses agree with the impedimetric measurements discussed earlier. The oxidation and reduction of electrolytic components on the bare gold electrode were characterized by a diffusion-limited transport kinetic with Ipa of 61.14 ± 0.35 μA. Diffusion limited for bare gold electrode was assumed considering the fact that redox active species with high electron transfer rate, such as the $[Fe(CN)_6]^{3-/4-}$ electrolyte, has an electron transfer rate controlled by the flow in which redox-active species are brought to the electrode surface (i.e. diffusion limited) [27]. Additionally, the voltammogram exhibits well-defined oxidative and reductive processes.

The electropolymerization of the pyrrole monomer caused an increase in the voltammetric signal. Additionally, the oxidation current became higher (Ipa = 141.06 ± 0.04 μA) due to polypyrrole-mediated electron transfer. A decrease in anodic and cathodic currents (Ipa = 77.27 ± 0.20 μA and Ipc = −64.98 ± 0.18 μA) was obtained after molecular structuring of the Chit-ZnONP nanocomposite on the PPy conductive matrix, indicating dielectric properties of the material. A lower voltammetric response (Ipa = 22.769 ± 0.255 μA) was observed after the chemical immobilization of DNA probes on the Chit-ZnONP composite. As expected, the use of BSA molecules to block nonspecific sites of the biosensor caused a reduction in voltammetric currents (Ipa = 18.432 ± 0.057 μA). Additionally, voltammetric and impedimetric characterizations for each isolated component that the biosensitive nanostructured platform was presented in Fig. S2. Therefore, it was possible to ensure the proper construction of the biological sensor on a transducer substrate through these electrochemical characterizations.

3.3. Evaluation of experimental conditions

3.3.1. Electrochemical polymerization of PPy

Fig. 3 shows the voltammetric measurements recorded during the potentiodynamic polymerization of pyrrole. Electropolymerization involves the application of a potential variation, resulting in the oxidation of the monomer unit. The electrochemical polymerization reaction proceeds with the coupling of monomer cations and oligomer cations until the PPy film is formed [28].

The electrochemical behavior of the electrode surface was

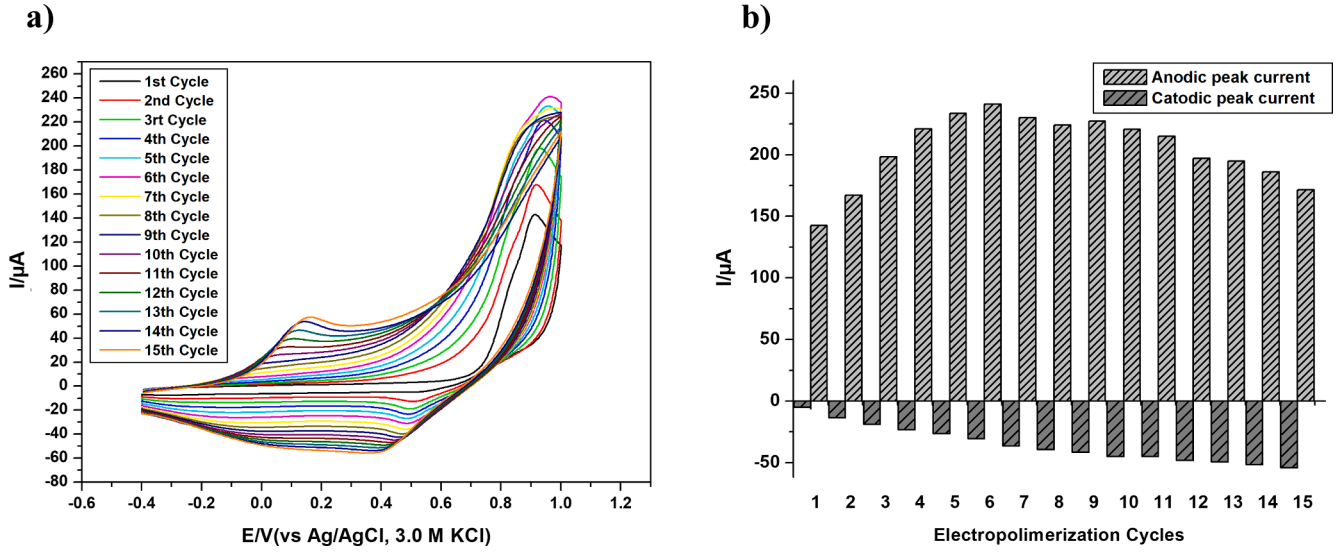

Fig. 3. Cyclic voltammograms (a) and peak currents (b) were recorded during the potentiodynamic polymerization of pyrrole.

investigated during 15 cycles of polymerization, where a reduction in the anodic current was observed after the 6th scanning cycle. This result is consistent with previous studies [29,30]. It is related to an increase in the conducting polymer layer resistance, lower electrical double layer capacitance, and decreased pyrrole monomers consumed during the synthesis [31]. Therefore, six electropolymerization cycles were ideal for obtaining a reproducible polymeric coating with maximum conductivity response and controllable thickness.

3.3.2. *Immobilization study of the Chit-ZnONP nanocomposite*

The self-assembled layer of Chit-ZnONP hybrid composite formed on a gold electrode previously modified with PPy was investigated under different adsorption times (1, 10, 20, 30, and 40 min). The increase in adsorption time resulted in voltammetric curves with anodic peak potential shifted to more positive potentials. This fact is due to the oxidation of zinc oxide species on the electrode surface [32] (Fig. 4a). According to Fig. 4b, the diameter of the impedance spectrum increased with the adsorption time. These responses indicate that the incubation period influences the amount of nanomaterial deposited on the transducer. Thus, it results in a change of the resistance signal. However, from the R_{CT} analysis (Fig. S3), it was verified that the time of 30 min causes electrodic saturation with moderate blocking of the redox reactions in the electrical double layer. Thus, the time of 30 min presented ideal adsorption kinetics for the molecular ordering of the Chit-ZnONP nanocomposite on the polymeric film.

3.4. *Analytical performance with plasmid DNA*

The detection study of the BCR/ABL chimeric oncogene involves monitoring variations in the electrochemical currents. The analytical behavior of the nanostrutured device was evaluated through the hybridization of recombinant plasmids. As evidenced in Fig. 5a, after exposing the PPy/Chit-ZnONP/Probe/BSA system to synthetic DNA samples, a reduction in the voltammetric signal was observed with a decrease in the height of the anodic and cathodic peaks. The electrochemical event indicates hybridization between two oligonucleotide strands, which causes greater electrostatic repulsion between the $[Fe(CN)_6]^{3-/4-}$ ions and the negatively charged phosphate groups of the gene molecules. Due to the formation of a barrier to electron transport, the current values are reduced with the more significant number of cDNA conjugates at the transducer interface [17].

Fig. 5b shows the anodic peak currents for the DNA biosensor after its exposure to different concentrations of the BCR/ABL chimeric sequence. The biodetection assay indicated that the proposed biosensor has an excellent linear response to BCR/ABL chimeric oncogene in the concentration range of 138.80 aM to 13.88 pM with a SD of 3.49 (Fig. 5b). The linear regression equation was expressed as $y = 12.07 - 1.06\ ^*\ln(x)$ with a coefficient of determination (R^2) of 0.96 (n = 6). Where *x* corresponds to the target DNA concentration and *y* refers to the Ipa value. It is noteworthy that the linearization of the *x* axis was performed on a logarithmic scale of the concentration. A LOD of 1.34 fM, LOQ of 4.08 fM, and sensitivity of 34.03 μA fM^{-1} cm^2 were estimated. These analytical variables were measured using the respective equations, 3.3SD/slope, 10SD/slope, and SD/(area of the electrode), where SD is the standard deviation of the blank sample (zero concentration) in triplicate and slope is the angular coefficient of the linearity study. The reproducibility for the bioanalysis system was 4.21%, obtained from the SD value for three independent biosensing tools produced with the same methodological process.

In addition, the percentage variation of the anodic peak current (ΔI), described as:

$$\Delta I(\%) = \frac{I_b - I_a}{I_b} \times 100 \quad (1)$$

was shown in Fig. S4. Where I_b and I_a correspond to the peak current before and after the oncogenic capture. A gradual increase in the ΔI (%) values can be seen in correlation with the concentration of the studied plasmids. The gene detection caused the linear variation of ΔI (%) from 33.62 ± 2.42% to 132.123 ± 3.84%, reflecting the molecular capture ability of the proposed system (Table S2).

3.5. *Electrochemical investigation in clinical samples*

Biodetection assays with real biological samples were performed to verify the clinical relevance of the nanostructured biosensor. Reduced voltammetric signals were reported in Fig. 6a after exposure of the sensing system to different cDNA samples from patients diagnosed with CML. Positive samples for BCR/ABL fusion gene caused significant current variations with ΔI values between 9.78 ± 3.62% and 561.44 ± 3.50% (Fig. 6b). Differences in the magnitude of the electrochemical responses can be attributed to the target oncogene expression and, consequently, to the staging of the hematologic malignancy [33]. These results indicate the feasibility of the sensor utilizing nanomaterials for gene screening in cDNA clinical specimens.

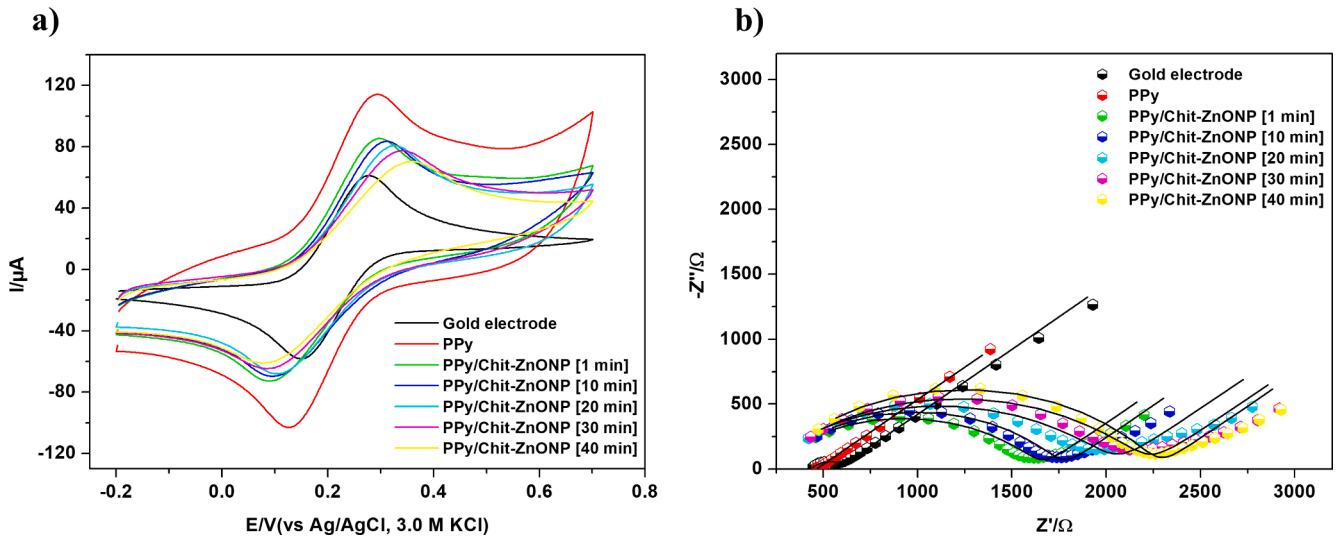

Fig. 4. Voltammetric plots (a) and impedance spectra (b) for the self-assembled layer of Chit-ZnONP hybrid composite formed under different adsorption times (1, 10, 20, 30, and 40 min). Three consecutive analyzes were conducted in each methodological procedure, where the experimental values are displayed as the mean values ± their standard deviation.

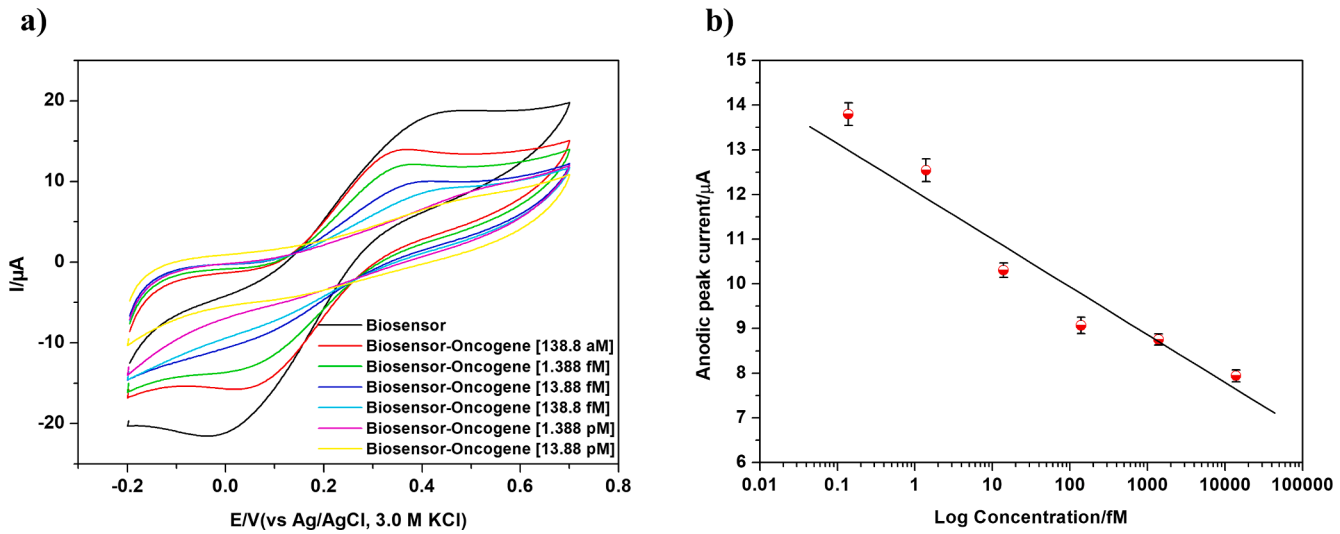

Fig. 5. Cyclic voltammograms (a) for the DNA biosensor exposed to variables concentrations of the BCR/ABL fusion gene in recombinant plasmids. Calibration plot of the bioanalytical platform with linear regression equation expressed as $y = 12.07 - 1.06\ ^{*}\ln(x)$, $R^2 = 0.96$, and SD = 3.49 (b). Three consecutive analyzes were conducted in each methodological procedure, where the experimental values are displayed as the mean values ± their standard deviation.

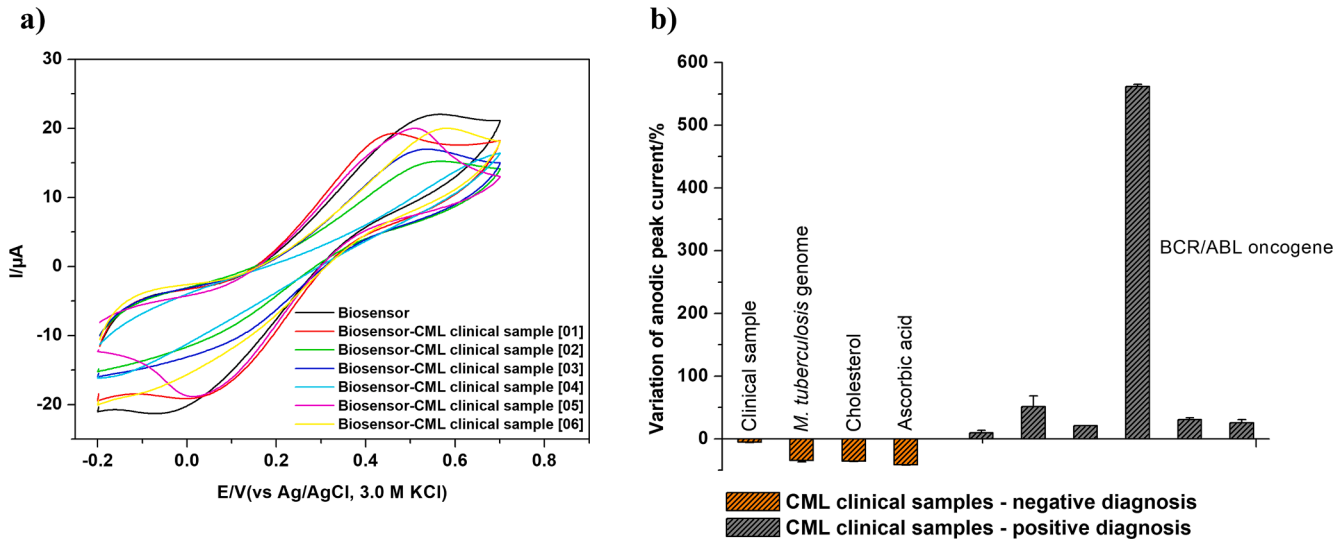

Fig. 6. Voltammetric records (a) of the DNA biosensor exposed to clinical samples from patients diagnosed with CML. The histogram shows ΔI values for the biosensor after assays with leukemia-negative samples and human cDNA samples containing biological interferers, such as *M. tuberculosis* genome, cholesterol (5 mM), and ascorbic acid (0.05 mM).

Specificity analysis was conducted using leukemia-negative samples. The interference studies were performed using human cDNA samples contained biological interferers: *Mycobacterium tuberculosis* genome, cholesterol (5 mM), and ascorbic acid (0.05 mM) [34]. The distinct electrochemical profiles show an excellent specificity and selectivity of the biosensor (Fig. 6b). Thus, the biosensor can be used for clinical trials with complex samples.

Conventional techniques for identifying genetic disorders in human blood have disadvantages such as late diagnosis, limited sensitivity, and and complex protocols. In contrast, the nanostructured biosensor developed in this study provides a fast analytical response within 15 min with a single hybridization step. Furthermore, the biodetection process occurs isothermally, at room temperature, without the need for temperature cycling, as in qRT-PCR experiments. In this perspective, a new tool developed for identification the BCR/ABL chimeric oncogene is relevant for the health promotion of patients with leukemia and the monitoring of minimal residual disease.

An analytical comparison with previous works is shown in Table 1. The biodevices presented in the Table 1 are based on the association of different nanomaterials, such as polyaniline nanostructures [18], ZnONPs [35], graphene sheets [36] and gold nanoparticles [17]. Electrodic modification methodologies were used to build biosensors on flexible or rigid transducers. It is observed that the use of conductive polymers such as polyaniline can increase the sensitivity of sensing tools, leading to limits of detection on the order of attomolar [18]. In this perspective, the incorporation of the Chit-ZnONP nanocomposite in a conductive matrix of PPy enabled the development of an innovative and biosensitive nanostructured platform, until then not described in electrochemical genosensors.

Distinctively from other studies, the developed bioanalysis system requires only small volumes of biological samples (only two microliters) for rapid and quantitative detection of the BCR/ABL fusion gene. The biodevice presented notable analytical performance parameters: comparable detection and quantification limits, high selectivity, and

Table 1
Analytical comparison between the biosensor presented in this work and the other DNA sensing systems reported in the literature for the electrochemical identification of the BCR/ABL fusion gene.

Sensor plataform	Electroanalytical technique	Limit of detection	Limit of quantification	Detection range	Response time	Electrochemical marker	Reference
ITO coated glass substrate / polyaniline nanotubes / biotinylated DNA probe	CV and EIS	0.1 fM	–	0.1 fM to 1 μM	20 min	–	[37]
ITO coated glass substrate / polyaniline-MoS_2 hybrid nanostructures / biotinylated DNA probe	CV and EIS	3 aM	–	10 aM to 1 μM	15 min	–	[38]
ITO coated glass substrate / amino-functionalized silica coated zinc oxide nanoparticles / aminated DNA probe	EIS	0.1 fM	–	0.1 fM to 1 μM	–	–	[35]
Glassy carbon electrode / graphene sheets / polyaniline / gold nanoparticles / thiolated DNA probe	CV, EIS and DVP	1.05 pM	–	10 pM to 20 nM	~ 90 min	Biotinylated hairpin molecules and streptavidin-labelled alkaline phosphatase	[36]
ITO electrode / 3D coral like polyaniline nanostructures / biotinylated DNA probe	CV and EIS	7 aM	–	10 aM to 1 μM	15 min	–	[18]
Glassy carbon electrode / gold nanoparticles / hemoglobin-capped gold nanoclusters stabilized graphene nanosheets / aminated DNA probe	CV, EIS and DVP	0.03 fM	–	aM to 10 pM	30 min	Methylene blue	[17]
Gold electrode / PPy / Chit-ZnONP / aminated DNA probe / BSA	CV and EIS	1.34 fM	4.08 fM	138.80 aM to 13.88 pM	15 min	–	This work

CV – cyclic voltammetry; DPV – differential pulse voltammetry; EIS – electrochemical impedance spectroscopy; ITO – indium tin oxide.

specificity. It is important to note that most electrochemistry-based assays require the analytical signal amplification using, for example, methylene blue, biotinylated hairpin molecules, and streptavidin-labelled alkaline phosphatase [17,36]. In this report, our DNA biosensor is label-free to reduce the demand for chemicals, response time, and methodological process costs.

4. Conclusions

The proposed biosensor is a promising tool for the molecular detection of the BCR/ABL chimeric oncogene. An innovative nanostructured platform based on PPy electropolymerized film and Chit-ZnONP nanocomposite was successfully obtained. The electrodic modification enabled amplification of the surface area, electron transfer efficiency, and biocompatible microenvironment. The biosensor is effective for leukemia investigation with high analytical performance, sensitivity, specificity, and selectivity. Small volumes of synthetic oligonucleotides and real biological samples were used in bioactivity assays. Thus, the biosensor can be applied for clinical trials. In addition, label-free electrochemical responses were measured at a 15-minute interval with limits of detection and quantification in the femtomolar order. Therefore, a new sensing assay was designed for diagnostic applications of hematologic malignancies, enabling the identification of early-stage cancer.

CRediT authorship contribution statement

Karen Y.P.S. Avelino: Methodology, Investigation, Formal analysis, Writing – original draft. **Léony S. Oliveira:** Methodology, Investigation, Formal analysis, Writing – original draft. **Maryana R. Santos:** Methodology, Investigation, Formal analysis, Writing – original draft. **Norma Lucena-Silva:** Conceptualization, Writing – review & editing, Supervision, Funding acquisition. **César A.S. Andrade:** Conceptualization, Writing – review & editing, Supervision, Funding acquisition. **Maria D. L. Oliveira:** Conceptualization, Writing – review & editing, Supervision, Funding acquisition.

Declaration of Competing Interest

The authors declare that they have no known competing financial interests or personal relationships that could have appeared to influence the work reported in this paper.

Acknowledgments

The researchers are grateful for the assistance provided by the Brazilian National Council for Scientific and Technological Development/CNPq (grant numbers 314894/2018-7 and 314756/2018-3); Brazilian Health Ministry Project DECIT-FINEP-CNPq (grant numbers 1299/2013 and 401700/2015-1); Pernambuco State Foundation for Research Support, FACEPE-PPSUS-APQ (grant number 0040-4.00/13); and PROPESQ/UFPE. Léony S. Oliveira and Sevy R.D.E. Oliveira would like to thank CAPES and CNPq for their respective scholarships.

Appendix A. Supplementary material

Supplementary data to this article can be found online at https://doi.org/10.1016/j.bioelechem.2022.108176.

References

[1] M. Baccarani, F. Castagnetti, G. Gugliotta, G. Rosti, A review of the European LeukemiaNet recommendations for the management of CML, Ann. Hematol. 94 (2015) 141–147.
[2] F. Loscocco, G. Visani, S. Galimberti, A. Curti, A. Isidori, BCR-ABL independent mechanisms of resistance in chronic myeloid leukemia, Front. Oncol. 9 (2019) 939.
[3] M.W. Deininger, N.P. Shah, J.K. Altman, E. Berman, R. Bhatia, B. Bhatnagar, D. J. DeAngelo, J. Gotlib, G. Hobbs, L. Maness, Chronic myeloid leukemia, version 2.2021, NCCN clinical practice guidelines in oncology, J. Natl. Compr. Canc. Netw. 18 (2020) 1385–1415.
[4] R. Ramchandren, T. Jazaerly, M.H. Bluth, A.M. Gabali, Molecular diagnosis of hematopoietic neoplasms: 2018 update, Clinics in Laboratory Medicine, 38 (2018) 293-310.
[5] X. Lu, M. Cui, Q. Yi, Detection of mutant genes with different types of biosensor methods, TrAC, Trends Anal. Chem. 126 (2020), 115860.
[6] A. Sabahi, R. Salahandish, A. Ghaffarinejad, E. Omidinia, Electrochemical nano-genosensor for highly sensitive detection of miR-21 biomarker based on SWCNT-grafted dendritic Au nanostructure for early detection of prostate cancer, Talanta 209 (2020), 120595.

[7] M.-B. Gholivand, A. Akbari, A sensitive electrochemical genosensor for highly specific detection of thalassemia gene, Biosens. Bioelectron. 129 (2019) 182–188.
[8] Z. Ait-Touchente, H.E.E.Y. Sakhraoui, N. Fourati, C. Zerrouki, N. Maouche, N. Yaakoubi, R. Touzani, M.M. Chehimi, High performance zinc oxide nanorod-doped ion imprinted polypyrrole for the selective electrosensing of mercury II ions, Appl. Sci. 10 (2020) 7010.
[9] S. Chawla, C.S. Pundir, An amperometric hemoglobin A1c biosensor based on immobilization of fructosyl amino acid oxidase onto zinc oxide nanoparticles–polypyrrole film, Anal. Biochem. 430 (2012) 156–162.
[10] N.P. Shetti, S.D. Bukkitgar, K.R. Reddy, C.V. Reddy, T.M. Aminabhavi, ZnO-based nanostructured electrodes for electrochemical sensors and biosensors in biomedical applications, Biosens. Bioelectron. 141 (2019), 111417.
[11] C. Singhal, C.S. Pundir, J. Narang, A genosensor for detection of consensus DNA sequence of Dengue virus using ZnO/Pt-Pd nanocomposites, Biosens. Bioelectron. 97 (2017) 75–82.
[12] Z. Hatami, E. Ragheb, F. Jalali, M.A. Tabrizi, M. Shamsipur, Zinc oxide-gold nanocomposite as a proper platform for label-free DNA biosensor, Bioelectrochemistry 133 (2020) 107458, https://doi.org/10.1016/j.bioelechem.2020.107458.
[13] H. Pyman, H. Roshanfekr, S. Ansari, DNA-based electrochemical biosensor using chitosan–carbon nanotubes composite film for biodetection of Pirazon, Eurasian, Chem. Commun. 2 (2020) 213–225.
[14] S. Mohajeri, A. Dolati, K. Yazdanbakhsh, Synthesis and characterization of a novel non-enzymatic glucose biosensor based on polyaniline/zinc oxide/multi-walled carbon nanotube ternary nanocomposite, J. Electrochem. Sci. Eng. 9 (3) (2019) 207–222.
[15] S.K. Shukla, A.K. Mishra, O.A. Arotiba, B.B. Mamba, Chitosan-based nanomaterials: A state-of-the-art review, Int. J. Biol. Macromol. 59 (2013) 46–58.
[16] N. Antony, S. Mohanty, S.K. Nayak, Electrochemical inspection of polypyrrole/chitosan/zinc oxide hybrid composites, J. Appl. Polym. Sci. 137 (2020) 49561.
[17] M. Shamsipur, L. Samandari, L. Farzin, F. Molaabasi, M.H. Mousazadeh, Dual-modal label-free genosensor based on hemoglobin@ gold nanocluster stabilized graphene nanosheets for the electrochemical detection of BCR/ABL fusion gene, Talanta 217 (2020), 121093.
[18] A. Soni, C.M. Pandey, S. Solanki, G. Sumana, Synthesis of 3D-coral like polyaniline nanostructures using reactive oxide templates and their high performance for ultrasensitive detection of blood cancer, Sens. Actuators, B 281 (2019) 634–642.
[19] J. Xia, J. Qing, J. Liu, A sensitive electrochemical impedance DNA biosensor based on ZnO nanorod electrodes for BCR/ABL fusion gene detection, Int. J. Electrochem. Sci 14 (2019) 4271–4279.
[20] R. Hoteit, R. Mahfouz, Proposed algorithm for the best detection of different bcr-abl gene fusion transcripts in molecular diagnostics laboratories: experience of a major referral center, Genet. Test. Mol. Biomarkers 15 (4) (2011) 227–229.
[21] L.-H. Li, J.-C. Deng, H.-R. Deng, Z.-L. Liu, L. Xin, Synthesis and characterization of chitosan/ZnO nanoparticle composite membranes, Carbohydr. Res. 345 (2010) 994–998.
[22] K. Rovina, S. Siddiquee, Electrochemical sensor based rapid determination of melamine using ionic liquid/zinc oxide nanoparticles/chitosan/gold electrode, Food Control 59 (2016) 801–808.
[23] J. Liu, D. Xuan, Z. Lu, Z. Wang, Q. Liu, S. Li, D. Wang, Y. Ye, D. Wang, Z. Zheng, A novel perspective on interfacial interactions between polypyrrole and carbon materials for improving performance of supercapacitors, Appl. Surf. Sci. 573 (2022), 151626.
[24] S. Carquigny, O. Segut, B. Lakard, F. Lallemand, P. Fievet, Effect of electrolyte solvent on the morphology of polypyrrole films: application to the use of polypyrrole in pH sensors, Synth. Met. 158 (2008) 453–461.
[25] F.G. Zamani, H. Moulahoum, M. Ak, D.O. Demirkol, S. Timur, Current trends in the development of conducting polymers-based biosensors, TrAC, Trends Anal. Chem. 118 (2019) 264–276.
[26] M.J. Jara-Palacios, M.L. Escudero-Gilete, J.M. Hernández-Hierro, F.J. Heredia, D. Hernanz, Cyclic voltammetry to evaluate the antioxidant potential in winemaking by-products, Talanta 165 (2017) 211–215.
[27] Y. Xing, S. O'Shea, S. Li, Electron transfer kinetics across a dodecanethiol monolayer self assembled on gold, J. Electroanal. Chem. 542 (2003) 7–11.
[28] A.A. Hermas, S.S. Al-Juaid, S.A. Al-Thabaiti, A.H. Qusti, M. Abdel Salam, In situ electropolymerization of conducting polypyrrole/carbon nanotubes composites on stainless steel: Role of carbon nanotubes types, Prog. Org. Coat. 75 (4) (2012) 404–410.
[29] K.Y. Avelino, L.S. Oliveira, N. Lucena-Silva, C.A. Andrade, M.D. Oliveira, Flexible sensor based on conducting polymer and gold nanoparticles for electrochemical screening of HPV families in cervical specimens, Talanta 226 (2021), 122118.
[30] K.Y. Avelino, G.S. Dos Santos, I.A. Frías, A.G. Silva-Junior, M.C. Pereira, M.G. Pitta, B.C. de Araújo, A. Errachid, M.D. Oliveira, C.A. Andrade, Nanostructured sensor platform based on organic polymer conjugated to metallic nanoparticle for the impedimetric detection of SARS-CoV-2 at various stages of viral infection, J. Pharm. Biomed. Anal. 206 (2021), 114392.
[31] M. Mahmoudian, W. Basirun, Y. Alias, A.K. Zak, Electrochemical characteristics of coated steel with poly (N-methyl pyrrole) synthesized in presence of ZnO nanoparticles, Thin Solid Films 520 (2011) 258–265.
[32] R. Renuka, L. Srinivasan, S. Ramamurthy, A. Veluchamy, N. Venkatakrishnan, Cyclic voltammetric study of zinc and zinc oxide electrodes in 5.3 M KOH, J. Appl. Electrochem. 31 (2001) 655–661.
[33] K.Y.P. dos Santos Avelino, I.A.M. Frías, N. Lucena-Silva, C.A.S. de Andrade, M.D. L. de Oliveira, Impedimetric gene assay for BCR/ABL transcripts in plasmids of patients with chronic myeloid leukemia, Microchim. Acta 185 (2018) 415.
[34] M.K. Patel, M.A. Ali, S. Srivastava, V.V. Agrawal, S. Ansari, B.D. Malhotra, Magnesium oxide grafted carbon nanotubes based impedimetric genosensor for biomedical application, Biosens. Bioelectron. 50 (2013) 406–413.
[35] C.M. Pandey, S. Dewan, S. Chawla, B.K. Yadav, G. Sumana, B.D. Malhotra, Controlled deposition of functionalized silica coated zinc oxide nano-assemblies at the air/water interface for blood cancer detection, Anal. Chim. Acta 937 (2016) 29–38.
[36] X. Chen, L. Wang, S. Sheng, T. Wang, J. Yang, G. Xie, W. Feng, Coupling a universal DNA circuit with graphene sheets/polyaniline/AuNPs nanocomposites for the detection of BCR/ABL fusion gene, Anal. Chim. Acta 889 (2015) 90–97.
[37] A. Soni, C.M. Pandey, S. Solanki, R. Kotnala, G. Sumana, Electrochemical genosensor based on template assisted synthesized polyaniline nanotubes for chronic myelogenous leukemia detection, Talanta 187 (2018) 379–389.
[38] A. Soni, C.M. Pandey, M.K. Pandey, G. Sumana, Highly efficient Polyaniline-MoS2 hybrid nanostructures based biosensor for cancer biomarker detection, Anal. Chim. Acta 1055 (2019) 26–35.